Transactions of the Korean Nuclear Society Autumn Meeting
Changwon, Korea, October 30-31, 2025

Axially-shielded Burnable Absorber (ABA) for Soluble Boron-Free SMR: Neutronics Feasibility in the Initial Cycle

Yunseok Jeong [a], Jaehyun Ryu [a], Dongju Choi [a], Young-June Lee [a], Yonghee Kim [a*]
[a]*Nuclear and Quantum Engineering, KAIST*
[*]*Corresponding author: yongheekim@kaist.ac.kr*

***Keywords :** Soluble boron-free, axially-shielded burnable absorber, SMR

1. Introduction

A soluble boron-free (SBF) small modular reactor (SMR) is a way of achieving advancements in both reactor design and safety margin. One of the main advancements in the reactor design is the simplification of chemical-volume-control-system (CVCS). Unlike the conventional nuclear reactors with soluble boron in their moderator, the boron-free SMR does not demand the complicated structures to control the soluble boron concentration in the moderator. On the safety margin side, the boron-free SMR enhances reactor safety by inherently avoiding boron dilution accidents. In such SBF cores, however, all excess reactivity must be suppressed using fixed burnable absorbers (BAs) and control rods. This places demanding requirements on BA performance: they must strongly reduce excess reactivity at beginning-of-cycle (BOC) while depleting nearly completely by end-of-cycle (EOC) to minimize reactivity penalties.

In light water reactors, gadolinium oxide (Gd_2O_3) has been widely adopted as a burnable absorber, typically mixed uniformly into selected fuel rods. Under SBF conditions, however, uniformly distributed gadolinia tends to deplete too rapidly, leading to a large initial reactivity drop and potential power peaking. To address these drawbacks, advanced BA geometries have been proposed. The Centrally-Shielded Burnable Absorber (CSBA) concept places gadolinia at the pellet center, where radial self-shielding slows gadolinium depletion and prolongs its effect [1], [2]. More recently, Highly Intensive Gadolinium/Alumina (HIGA) rods, introduced by Kim et al. at KNF, demonstrated that a small number of gadolinia-rich rods can effectively control reactivity in the i-SMR core while maintaining acceptable power profiles [3]. These studies emphasize that self-shielding geometry is essential for reliable boron-free reactivity control.

Building on these developments, this study proposes the Axially-shielded Burnable Absorber (ABA) concept. Unlike CSBA or HIGA, which focus on radial or discrete absorber arrangements, ABA employs conventional Gd_2O_3-bearing fuel rods but introduces their axial segmentation within the fuel assembly. By placing gadolinia-loaded fuel in selected axial regions, the natural neutron flux gradient along the core height provides an effective self-shielding mechanism, slowing gadolinium depletion over the cycle. This configuration is intended to maintain effective reactivity control throughout the initial cycle while ensuring that the absorber material is nearly burned by end-of-cycle. Importantly, ABA relies solely on well-established Gd_2O_3 fuel technology, avoiding the need for new fabrication processes.

The objective of this work is to evaluate the neutronics feasibility of ABA in the initial cycle of the i-SMR core proposed by KNF (2024). Using the continuous-energy Monte Carlo code Serpent 2 [4], we analyze reactivity swing, power peaking, and axial power distribution.

2. Methods

The reference core design adopted in this study preserves the thermal output, number of fuel assemblies, coolant inlet and outlet temperatures, and reflector composition of the baseline design in [3], while modifying the fuel enrichment and absorber configuration to investigate the proposed concept. The core is divided into four radial fuel-enrichment zones. As illustrated in Figure 1, the fuel enrichment is graded as 2.9, 3.0, 3.5, and 4.0 wt% U-235 from the outermost to the innermost region. The figure shows a one-eighth sector of the core with E5 representing the core center.

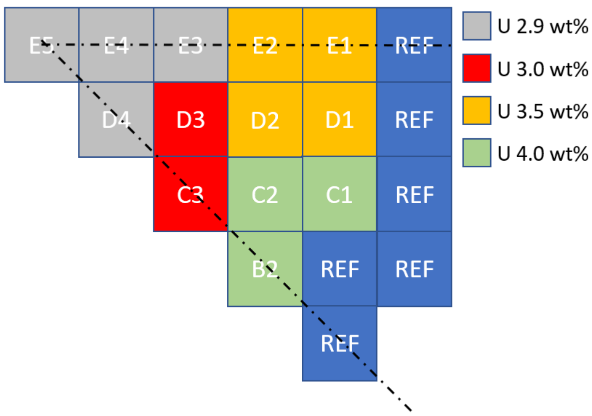

Figure 1 Radial zoning of the core (1/8 shown).

The Axially-shielded Burnable Absorber (ABA) is implemented by inserting gadolinia-bearing fuel layers of 1 cm thickness at specific axial positions of every fuel rod within an assembly. Each absorber layer contains

UO_2 fuel uniformly mixed with Gd_2O_3 at a designated weight fraction. Unlike conventional homogeneous gadolinia loading, the ABA arrangement combines multiple absorber categories to achieve both long-term and early-cycle reactivity suppression.

Three absorber categories are defined in the ABA using core. The primary BA layers (seven in total) are located at 37–38, 65–66, 92–93, 118–119, 145–146, 173–174, and 201–202 cm along the active core height. With the highest gadolinia concentrations (16 wt% in the Inner Zone and 15 wt% in the Boundary Zone), they are strongly self-shielded, such that a significant fraction of the absorber remains unburned until near the end of cycle (EOC). This design intentionally provides sustained suppression of excess reactivity over the full cycle, avoiding a late-cycle reactivity upswing.

The secondary BA layers (six in total, at 51–52, 79–80, 105–106, 131–132, 159–160, and 187–188 cm) are also aimed at long-term control, gradually compensating for the primary BA depletion. Their gadolinia concentrations are 11 wt% in the Inner Zone and Boundary Zone, shaping the mid-cycle reactivity swing and ensuring a smooth axial power distribution.

The tertiary BA layers (four in total, at 11–12, 23–24, 215–216, and 228–229 cm) use relatively low gadolinia concentrations (1.5–8–7–1.5 wt% in both zones). Tertiary BA using 1.5 wt% gadolinia concentrations are primarily intended to suppress the initial excess reactivity during the early stage of operation, but are designed to fully deplete within roughly the first 300 days. This prevents over-suppression of reactivity when other highly concentrated gadolinias are not burned enough. The complete radial–axial absorber layout is shown schematically in Figure 2.

Fuel enrichment in ABA region is determined according to the Eq. (1) below:

$$4.65 \times (1 - 0.05 \times wt\%) \quad (1)$$

All neutronics calculations were performed with the continuous-energy Monte Carlo code Serpent 2 [4], which enables detailed three-dimensional modeling of the ABA configuration and burnup-dependent depletion. In the Monte Carlo simulations, the axial variation of coolant temperature was explicitly considered, reflecting the temperature rise along the flow direction. The inlet coolant temperature was set to 568.7 K, and the outlet coolant temperature was adjusted to 593.15 K, resulting in an axial coolant temperature gradient across the active core. The fuel temperature was assumed to be spatially uniform at 903 K.

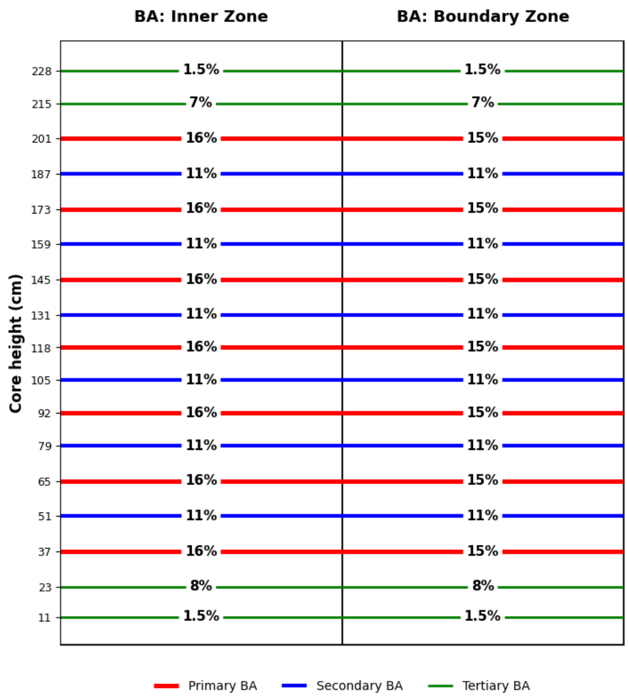

Figure 2 Axial distribution of ABA layers: Red: 1st BA, Blue: 2nd BA, Green 3rd BA. Each layer corresponds to 1 cm of gadolinia-bearing fuel.

On the basis of the power distributions obtained from Serpent 2, a two-dimensional thermal-hydraulic analysis of a representative hot channel was carried out using COMSOL Multiphysics. The hot channel model was constructed in an R–Z cylindrical geometry with the equivalent hydraulic diameter applied to represent the coolant subchannel. The Serpent-derived axial and radial power profiles were applied as input heat sources to the COMSOL model, which allowed for evaluation of the fuel centerline temperature under nominal operating conditions.

3. Numerical Results

Figure 3 shows the evolution of the multiplication factor during the initial core cycle. With the ABA configuration, the excess reactivity remains within about 1200 pcm throughout the entire burnup range. This demonstrates that the absorber arrangement effectively suppresses the large initial excess reactivity while avoiding any significant mid- or late-cycle reactivity rise. The design target cycle length was approximately 720 EFPD, and the results show that the achieved cycle length is very close to this target. Overall, the ABA configuration achieves a controlled reactivity swing, supporting stable operation across the entire cycle.

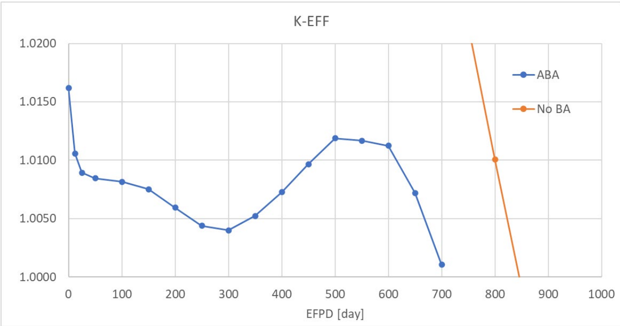

Figure 3 Multiplication factor.

Figure 4 presents the axial power distribution at BOC. The profile remains nearly symmetric along the core height, even when considering the effect of the negative moderator temperature coefficient (MTC). This behavior is attributed to the deliberate adjustment of the BA layer spacing: in the upper region, the BA layers are positioned slightly less concentrated toward the center, which prevents the power distribution from being skewed to one side. As a result, the axial power shape is well-balanced, with localized dips at the absorber layer positions due to strong absorption and a controlled local peak of about 1.43 observed near the 70 cm position.

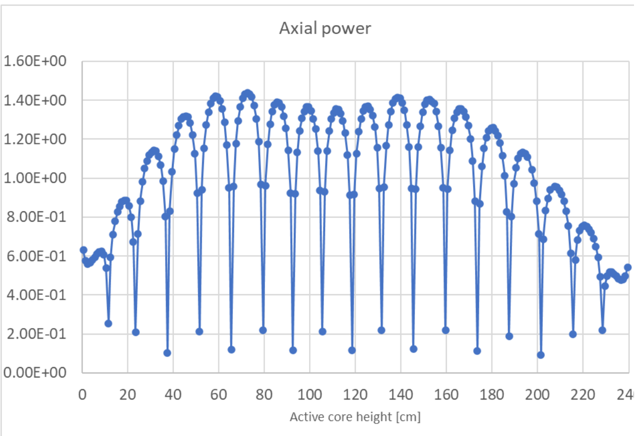

Figure 4 Axial power distribution at BOC.

Figure 5 presents the radial power distribution at BOC. The highest power is observed in assembly E2, where the peaking factor reaches approximately 1.17, while the core center (E5 assembly) shows slightly lower power. This result demonstrates that the applied radial enrichment zoning effectively shifts power away from the center and yields a reasonably flat radial distribution.

1.11E+00	1.13E+00	1.15E+00	1.17E+00	7.85E-01
	1.14E+00	1.17E+00	1.16E+00	7.64E-01
		1.15E+00	1.15E+00	6.73E-01
			8.03E-01	REF

Figure 5 Radial power distribution at BOC.

Figure 6 shows the axial power distribution at 300 EFPD (MOC). By this point in the cycle, the tertiary burnable absorbers with lower gadolinia weight fractions have been almost completely depleted, while the absorbers with 8% and 7% gadolinia still remain active. This indicates that the lower-weight-fraction absorbers deplete faster than those in the higher-weight-fraction central region, thereby successfully preventing excessive power rises at the core bottom and top ends. As a result, the axial power profile remains well controlled, with a peak of about 1.3 observed near the 30 cm region. Distinct local dips still coincide with the primary and secondary absorber layers, confirming the continued effectiveness of the absorber arrangement in flattening the power shape and long-term reactivity suppression.

Figure 7 presents the corresponding radial power distribution at 300 EFPD. The highest power is observed at the core center (E5 assembly), where the peaking factor reaches about 1.25.

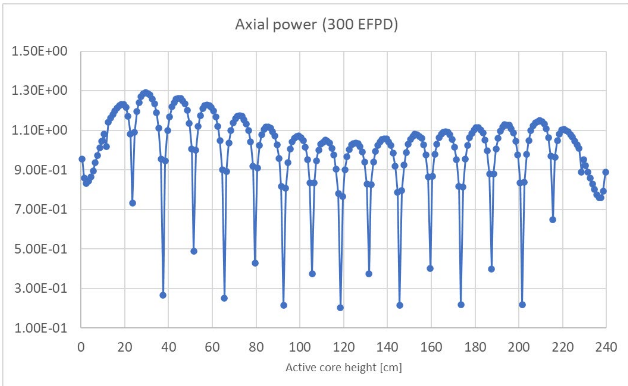

Figure 6 Axial power distribution at MOC.

1.25E+00	1.24E+00	1.20E+00	1.14E+00	7.63E-01
	1.22E+00	1.19E+00	1.11E+00	7.28E-01
		1.12E+00	1.04E+00	6.21E-01
			7.29E-01	REF

Figure 7 Radial power distribution at MOC.

Figure 8 shows the axial power distribution at EOC (≈700 EFPD). At this stage, most of the gadolinia has been fully depleted, and the axial power profile has converged to a nearly cosine-like shape. The axial peak appears at about 1.25 in the core center, which remains within an acceptable operational margin. Local depressions are still visible at the absorber layer positions, but these are now primarily caused by the reduced U-235 enrichment in those regions rather than residual gadolinia absorption. The impact of these dips on the global power distribution is minor, indicating that the end-of-cycle power shape is well balanced and consistent with expectations.

Figure 9 presents the corresponding radial power distribution at EOC. The maximum radial peaking is observed at the D3 assembly, reaching about 1.21, indicating that the radial power profile is well flattened despite the complete depletion of absorbers.

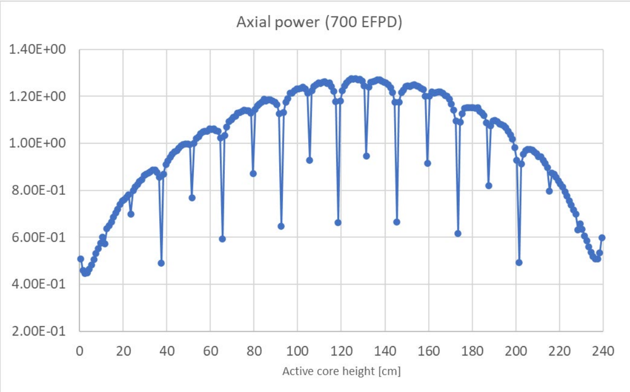

Figure 8 Axial power distribution at EOC.

1.14E+00	1.16E+00	1.18E+00	1.17E+00	8.08E-01
	1.18E+00	1.21E+00	1.15E+00	7.79E-01
		1.17E+00	1.10E+00	6.56E-01
			7.72E-01	REF

Figure 9 Radial power distribution at EOC.

To further assess thermal margins, a representative hot channel calculation was performed at MOC (≈300 EFPD) using COMSOL Multiphysics, based on the power distribution obtained from Serpent 2. The hot channel was defined by multiplying the radial and axial peaking factors at MOC, with an additional factor of 1.05 applied to account for intra-assembly pin power peaking. The thermal conductivity of gadolinia-bearing regions was modeled using UO_2–Gd_2O_3 mixed-fuel correlations [5]. For conservative numerical analysis, however, the conductivity of all fuel regions was assumed to be that of UO_2–Gd_2O_3 fuel with 8 wt% gadolinia, thereby underestimating the heat conduction capability and ensuring a highly conservative evaluation of thermal margins.

Figure 10 shows the resulting temperature distribution along the core height. Even under this conservative assumption, the maximum fuel centerline temperature is limited to approximately 1560 K, occurring near the lower end of the core. In the mid-core region, the centerline temperature remains around 1300–1350 K, with distinct local depressions at the axial positions where burnable absorbers were loaded, reflecting the reduced local fission power generation. These results confirm that, even with the highly conservative conductivity assumption, the predicted fuel centerline temperature remains sufficiently low.

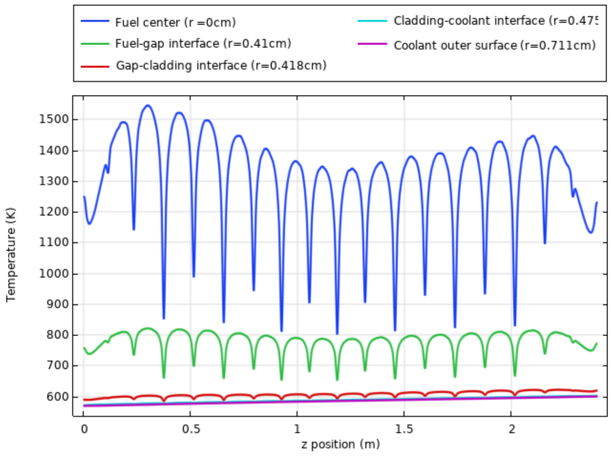

Figure 10 Fuel centerline and coolant outer-surface temperatures in the representative hot channel at MOC.

4. Conclusions

This study evaluated the neutronic feasibility of the Axially-shielded Burnable Absorber (ABA) concept for a soluble-boron-free SMR core during the initial cycle, using gadolinia-bearing fuel with radial enrichment zoning and zoned BA loading between inner and boundary assemblies. The ABA configuration effectively suppresses the initial excess reactivity, keeping it within 1200 pcm throughout most of the cycle, and supports a cycle length of about 720 EFPD. By EOC, gadolinium burnout yields a nearly cosine-like axial power profile with a peak of about 1.25, and the radial profile remains well flattened with a maximum peaking factor of about 1.21 at the D3 assembly region.

Hot-channel analysis at MOC, performed using COMSOL with conservative assumptions that all fuel regions follow the thermal conductivity of UO_2–Gd_2O_3 mixed-fuel at 8 wt% gadolinia, predicted a peak fuel centerline temperature of ~1560 K near the lower end of the core and ~1300–1350 K in the mid-plane. Local depressions were observed at BA-loaded layers, reflecting reduced local power generation. While these results confirm that fuel centerline temperatures remain well below safety thresholds.

Overall, the ABA concept demonstrates potential as a gadolinia-only solution for soluble-boron-free operation, but further refinement is required. In particular, optimization of gadolinia concentration, absorber layer phasing, and end-zone enrichment—together with explicit coupling to thermal–hydraulic feedback—will be essential to mitigate MOC end-peaking and secure robust thermal margins. In addition, extending the analysis to multi-cycle operation and pursuing strategies to minimize power peaking throughout the cycle represent important next steps toward establishing the practicality of the ABA design.

REFERENCES

1. X. H. Nguyen, C. H. Kim, and Y. H. Kim, "An advanced core design for a soluble-boron-free small modular reactor ATOM with centrally-shielded burnable absorber," Nuclear Engineering and Technology, vol. 51, no. 2, pp. 369–376, Feb. 2019, doi: 10.1016/j.net.2018.11.016.
2. S. Wijaya, X. H. Nguyen, Y. Jeong, and Y. H. Kim, "Multi-batch core design study for innovative small modular reactor based on centrally-shielded burnable absorber," Nuclear Engineering and Technology, vol. 56, no. 3, pp. 907–915, Mar. 2024, doi: 10.1016/j.net.2023.11.007.
3. J. S. Kim, et al., "Highly Intensive Gadolinium/Alumina (HIGA) burnable absorber rods for soluble-boron-free i-SMR core," in Proc. Korean Nuclear Society Spring Meeting, 2024.
4. J. Leppänen, M. Pusa, T. Viitanen, V. Valtavirta, and T. Kaltiaisenaho, "The Serpent Monte Carlo code: Status, development and applications in 2013," Annals of Nuclear Energy, vol. 82, pp. 142–150, Aug. 2015, doi: 10.1016/j.anucene.2014.08.024.
5. Ohira K. and Itagaki N. "Thermal Conductivity Measurements of High Burnup UO2 Pellets and Benchmark Calculation of Fuel Center Temperature.", *Proceedings of the ANS International Topical Meeting on LWR Fuel Performance*, pp. 541-549. March 2-6, 1997, Portland, OR.